

Article

# Multifunctional Surface Modification of Mulberry Silk Fabric via PNIPAAm/Chitosan/PEO Nanofibers Coating and Cross-Linking Technology

Jia Li <sup>1,2,†</sup>, Boxiang Wang <sup>1,2,†</sup>, Jie Lin <sup>1,2</sup>, Dehong Cheng <sup>1,2,\*</sup> and Yanhua Lu <sup>1,2,\*</sup>

<sup>1</sup> Liaoning Provincial Key Laboratory of Functional Textile Materials, Eastern Liaoning University, Dandong 118000, China; lj18840597623@163.com (Jia.L.); bxwang0411@163.com (B.W.); linjieln@163.com (Jie.L.)

<sup>2</sup> School of Chemical Engineering, Eastern Liaoning University, Dandong 118003, China

\* Correspondence: 13470016052@163.com (D.C.); yanhualu@aliyun.com (Y.L.)

† These authors contributed equally to this work.

Received: 8 December 2017; Accepted: 5 February 2018; Published: 9 February 2018

**Abstract:** Multifunctional mulberry silk fabrics with excellent temperature- and pH-sensitivity, antibacterial properties and permeability are successfully prepared by surface modification with PNIPAAm/chitosan/poly(ethylene oxide) nanofibers. The nanofibers deposited on the surface of mulberry silk fabric are produced by the electrospinning technique. The surface properties of mulberry silk fabrics were changed by coating process and glutaraldehyde vapor cross-linking technology. The PNIPAAm/chitosan/PEO nanofibers have good apparent morphology and uniform fiber diameter. The contact angle of modified mulberry silk obviously increases with the increasing temperature. The bacterial reduction rates of modification of mulberry silk against *E. coli* and *S. aureus* all reach above 80%. Permeability test results show that it can largely improve the poor permeability of coated fabric by intelligent nanofiber modification technology. The air permeability of temperature- and pH-sensitivity mulberry silk fabric modified with PNIPAAm/chitosan/PEO nanofibers, which has reached about  $5.1 \times 10^2$  L/m<sup>2</sup>/s, is higher than that of the silk fabric coated with PNIPAAm/chitosan/PEO solution that reached  $1.5 \times 10^2$  L/m<sup>2</sup>/s. The nanofibers coated with mulberry silk fabrics show outstanding temperature- and pH-sensitivity, antibacterial properties and permeability, and may be a potential application in medical care, intelligent materials and textiles.

**Keywords:** chitosan; poly(*N*-isopropyl acrylamide); mulberry silk; electrospinning; antibacterial activity; thermosensitive behavior

## 1. Introduction

In the past decades, many research works have been dedicated towards the modification silk functionalization, both in industrial and academic circles, aiming at imparting new and high performance functions to the silk fabrics. For this purpose, great efforts have been devoted to the surface modification of silk fabrics in order to control its properties, such as crease recovery, dyeing ability, color fastness, or hydrophobicity [1–4]. A particular interesting strategy would be to graft stimuli-responsive polymers that would turn silk textiles into a smart material that responds to changes in the environment, e.g., temperature, pH or light. The emerging applications of stimuli-responsive polymers have a large potential and have attracted much interest [5–9].

Currently, the most attractive ways to modify surfaces with polymer is to perform surface-initiated polymerization via a “grafting from” approach that can be used to polymerize poly(*N*-isopropylacrylamide) (PNIPAAm) brushes. PNIPAAm is a well-known thermoresponsive polymer that shows an extended hydrophilic chain conformation below its lower critical solution temperature in aqueous solution and undergoes a phase transition to insoluble and hydrophobic aggregates when temperature is above its lower

critical solution temperature [10]. In most of these cases, as well as for the majority of textiles modified surfaces, the responsive polymer was worked into the textile surfaces by surface coating technology to perform its characterization. However, most of the fabric modified by the surface coating technology was of the hard-feeling, and had poor air permeability and so on [11–13]. At that time, the electrospinning technology was not yet applied to the fabric surface modifications.

Electrospinning is a simple, versatile, and effective approach to fabricate nanofibers from various synthetic and natural polymers [14–16]. To date, various nanofibers produced by electrospinning have been applied successfully in many fields, for example, tissue engineering, biotechnology, environmental engineering, filters, and sensors [17–20].

Chitosan, as a most important natural polymer of marine crustaceans, shrimp and crabs, is good biocompatibility and biodegradability [21,22]. Much of the potential of chitosan as a biomaterial stems from its cationic nature and high charge density in solution. The charge density allows chitosan to form insoluble ionic complexes or complex coacervates with a wide variety of water-soluble anionic polymers. This property can be used as a technique for local delivery of biologically active, especially textile finishing area [23]. As the functional “green” textile finishing agent, chitosan is abundantly present in textile engineering chitosan [24,25].

In this work, the PNIPAAm polymer was primarily prepared by the initiator method and then an extensive study was performed to characterize—in situ—the structure and characteristics of the PNIPAAm brushes directly grown from the surface of silk fabric, while still connected to the substrate. Then, the aqueous solution of chitosan was mixed with PNIPAAm to obtain the temperature response. Then, the above-mixed solution was blended with poly(ethylene oxide) (PEO) solution to improve the electrospinnability of the PNIPAAm/chitosan. We suggested a modified method that the blend PNIPAAm/chitosan/PEO nanofiber mat was used to modify the mulberry silk fabric to form the smart silk fabric, which endowed the mulberry silk with temperature- and pH-response. The chemical and structural characteristics of the PNIPAAm/chitosan/PEO nanofiber mat and the modified mulberry silk fabrics were studied and compared with other samples. Moreover, the biological performance of the modified mulberry silk fabrics was investigated by an antimicrobial activity experiment.

## 2. Experimental

### 2.1. Materials

*N*-isopropylacrylamide (NIPAAm, 98%) and *N,N,N,N*-tetramethylethylenediamine (TMEDA) was purchased from Aladdin Reagent (Shanghai, China). Ammonium peroxodisulfate (APS) was obtained from Sinopharm Chemical Reagent Co., Ltd. (Shenyang, China) Chitosan (chitosan, 98% degree of deacetylation), Glutaric dialdehyde (GA) (25%) and acetic acid (99%) were obtained from Kermel Reagent (Tianjin, China). *N,N*-methylenebisacrylamide (BIS) was supplied by Shanghai Bio-Technology Co., Ltd. (Shanghai, China).

### 2.2. Preparation of the Hydrogel and Spinning Solution

The NIPAAm monomer (1.0 g) and BIS (40.0 mg) were dissolved in distilled water to prepare 6.5 wt % monomer solution. The chitosan (1.0 g) was dissolved in acetic acid to form 2.5 wt % chitosan acetic acid solution, and then being mixed with monomer solution for 30 min. TMEDA (6.0 mg)/APS (6.0 mg) served as a redox initiator were mixed in the polymerization solution and stirred for 30 min to obtain the PNIPAAm/chitosan hydrogel.

PEO (MW = 60 kDa) power (1.5 g) was dissolved in 100 mL distilled water under continuous magnetic stirring at 45 °C for about 4 h to prepare 15 wt % PEO solution. The NIPAAm/chitosan hydrogel was dissolved in PEO solution to prepare the PNIPAAm/chitosan/PEO (15/45/40, 20/40/40, 25/35/40, 30/30/40, 35/25/40) (*v/v/v*) blend spinning solution.

### 2.3. Fabrication of Electrospun Nanofibers

Electrospinning was performed using electrospinning machines (KH08, Jinan Liangrui Technology Co., Jinan, China) with a horizontal set up containing a high DC voltage power supply and a syringe pump. All the electrospinning experiments in this study are at room temperature, humidity of about 65%. The electrospinning process was performed at 20 kV applied voltage, 15 cm working distance, and 0.03 mL/h flow rate. The nanofiber mats were produced with a deposition time of 30, 60, and 90 min.

### 2.4. Functionalization of Mulberry Silk

The silk fabric was soaked in glutaraldehyde solution for 30 min and then fixed on the cylinder. The PNIPAAm/chitosan/PEO nanofibers were manufactured from the primary PNIPAAm/chitosan/PEO spinning solution, while the functional mulberry silk was prepared by the further crosslinked on the glutaraldehyde vapor condition at room temperature for 24 h. The scheme of the of functional mulberry silk is shown in Figure 1.

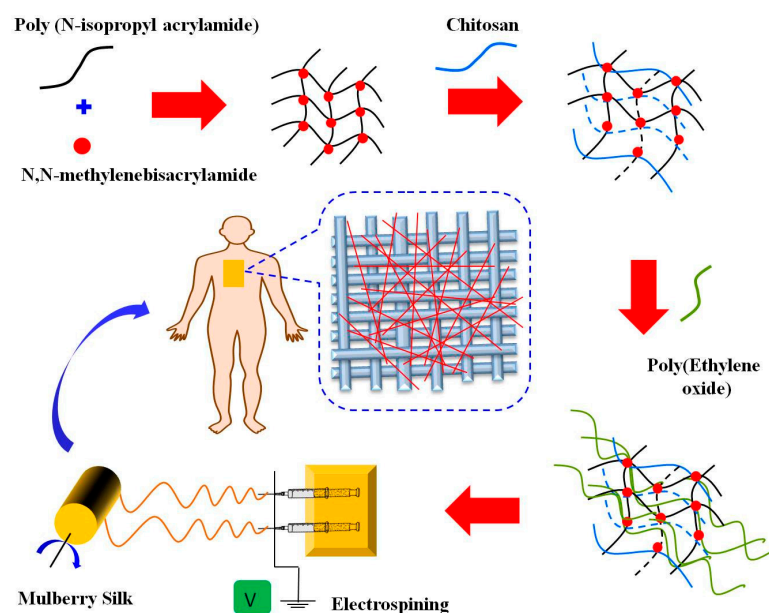


**Figure 1.** Scheme process of prepared the temperature- and pH-sensitivity mulberry silk fabric.

### 2.5. Characterization

#### 2.5.1. Hydrogel pH-Responsive Swelling Behaviors

The 4 groups of PNIPAAm/chitosan hydrogels were immersed for 24 h in various pH buffers and dried in vacuo at room temperature for 24 h. The swelling degree ( $q$ ) was calculated as follows [26]:

$$q = \frac{W_s - W_d}{W_d} \quad (1)$$

where  $W_d$  and  $W_s$  are the masses of the dried and fully hydrated hydrogel, respectively.

#### 2.5.2. Hydrogel Thermosensitive Behavior Measurements

For each PNIPAAm/chitosan hydrogel, the 4 groups of swelling hydrogel was injected in the shape of 10 mm × 10 mm × 40 mm cuvette. The temperature was raised from 25 to 60 °C, and every test temperature was stabilized for 5 min before analysis. The transmittance at 500 nm was measured using a 723 UV-Vis spectroscopy (APL Instruments Shanghai Co., Ltd., Shanghai, China).

### 2.5.3. Scanning Electron Microscopy

The morphologies of the mulberry silk fabric and nanofiber mats were analyzed using a scanning electron microscope (SEM, JSM-IT100, JEOL, Tokyo, Japan).

### 2.5.4. Fourier Transform Infrared Spectroscopy

The properties of the secondary structure and degree of crystallinity of NIPAAm, chitosan, PNIPAAm, PNIPAAm/chitosan/PEO nanofibers and the mulberry silk, intellectualized mulberry silk were characterized by Fourier-transform infrared spectroscopy (FT-IR, Tensor-37, Bruker, Karlsruhe, Germany).

### 2.5.5. Fabric Contact Angle Measurements

The contact angle of water was measured using angle measurements (PT-705, PST International Equipment Co., Ltd., Dongguan, China), and the contact angle values were recorded after 3 s when the water drop began to still on the silk fabric.

### 2.5.6. Fabric Air Permeability Measurements

Air permeability of the the mulberry silk fabric was examined using Air Permeability Tester (FX 3300 LabAir IV, Lippo Science Equipment Co., Ltd., Shanghai, China).

### 2.5.7. Fabric Antimicrobial Activity Measurements

The antibacterial activity was quantitatively evaluated against *Staphylococcus aureus* (ATCC 6538) and *Escherichia coli* (ATCC 8739), according to the AATCC 100 test method and GB/T 31713-2015 [27]. The 3 groups of fabric samples with  $4.8 \pm 0.1$  cm diameter were placed in a 50 mL conical flask and inoculated with 0.5 mL of bacterial culture. After incubation over contact periods of 24 h, the solution was serially diluted. The diluted solution was plated on nutrient agar and incubated for 24 h at  $37 \pm 2$  °C. Colonies of bacteria recovered on the agar plate were counted and the percent reduction of bacteria ( $R$ ) was calculated by the following equation:

$$R = \frac{A - B}{A} \times 100\% \quad (2)$$

where  $R$  is the reduction (%),  $B$  is the number of bacteria recovered from the inoculated treated test specimen swatches in the jar incubated over the desired contact period, and  $A$  is the number of bacteria recovered from the inoculated treated test specimen swatches in the jar immediately after inoculation (at "18 h" contact time).

## 3. Results and Discussion

### 3.1. pH-Responsive Swelling Behaviors

Figure 2 illustrates the swelling degree of PNIPAAm/chitosan hydrogel against the various pH buffers. Below pH = 6, the hydrogel swelled up to 3.5 times. The swelling of the hydrogel increased significantly, up to 5 times, at pH = 7, and then continued more gradually as the value of pH increased to 8. At pH = 10, the swelling of hydrogel collapsed to levels slightly above those above at pH = 8.

This observation implied that the swelling of the PNIPAAm/chitosan hydrogel was responsive to the ionic strength as well. The swelling transitions were caused by the ionization of carboxylic acid groups and ammonium group on hydrogel [28]. The interaction between  $-\text{NH}^+$  group and  $-\text{COO}^-$  group in acidic buffer solution moves weakened as the gradually decreased pH. This is because the carboxylic acid groups are mainly exist in the form of  $-\text{COOH}$  group in acidic buffer solution. However, the hydrogen bonds between  $-\text{NH}^+$  group and  $-\text{COO}^-$  group with water deseparately enhanced and the swelling degree markedly improved as the increased pH [29,30].

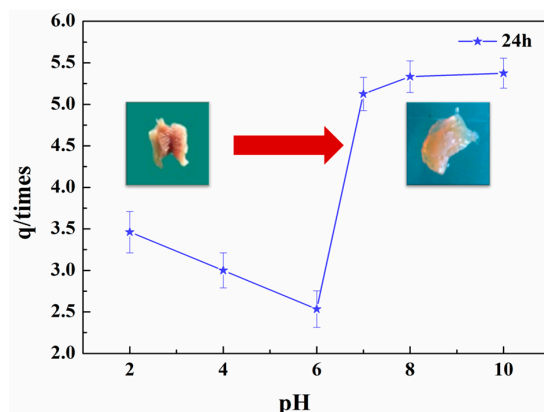


**Figure 2.** The pH-responsive swelling behaviors of PNIPAAm/chitosan hydrogel (at pH = 2–10) (swelling for 24 h in each buffer). Data are presented as mean  $\pm$  standard deviation.

### 3.2. Thermosensitive Behavior

The schematic illustration of the hydrophilic–hydrophobic phase transition of PNIPAAm was shown in Figure 3. In this temperature range, which is below LCST (the lower critical solution temperature) (LCST = 33 °C), PNIPAAm interacts preferentially with solvent molecules and adopts an extended configuration. With the increasing temperature, PNIPAAm molecules gradually turn into the hydrophobic state forming hydrogen bond. The mobility of each molecule is therefore seriously restricted by the hydrogen-bonded polymer networks. At the higher temperature region, the hydrophilic–hydrophobic transition has finished, and the slow increase of aliphatic resonance intensity is attributed to the increased molecular mobility at elevated temperature.

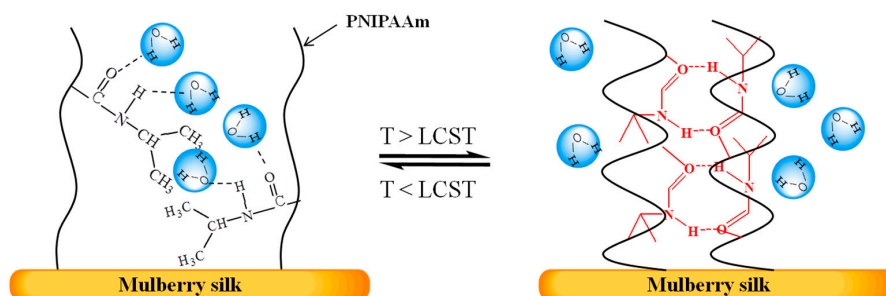


**Figure 3.** Schematic illustration of the hydrophilic–hydrophobic phase transition.

The transmittance curves in Figure 4a suggest that of PNIPAAm/chitosan hydrogel showed an obvious phase transition. The results show that the transmissivity of the sample decrease with the increasing temperature. The LCST was defined as the temperature at the highest point of the derivation curve of transmittance vs. temperature. The data indicated that the LCST of PNIPAAm/chitosan hydrogel was about 33 °C after curve fitting [31]. This indicates that the chitosan did not chemically react with the *N*-isopropylacrylamide. And the thermosensitive behavior of the PNIPAAm/chitosan hydrogel is shown in Figure 4b. The phase transition of PNIPAAm/chitosan hydrogel gradually changes from the colorless transparent to white with the increasing temperature. When the temperature is about 33 °C, the color of PNIPAAm/chitosan hydrogel is almost totally white quite, as suggested by the analysis of the transmittance curves [32–34].

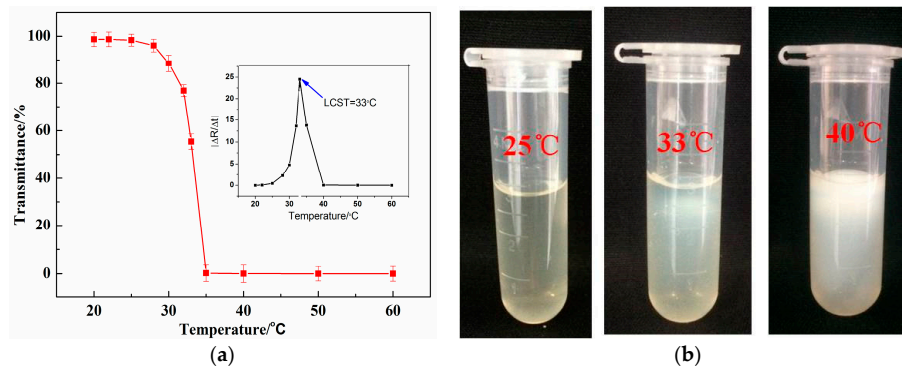


**Figure 4.** Thermosensitive behavior of the PNIPAAm/chitosan hydrogels: (a) Temperature dependence for the optical transmittance; (b) Photograph of the hydrogels at different temperatures. Data are presented as mean  $\pm$  standard deviation.

The DSC (differential scanning calorimetry) thermogram curves in Figure 5 suggest that of PNIPAAm/chitosan hydrogel showed an obvious phase transition. In this research work, the LCST of PNIPAAm/chitosan hydrogel was accurately determined using differential scanning calorimetry (DSC, 200F3, Netzsch, Selb, Germany). The onset temperature was considered as the LCST value, which was determined by the intersection point of the two tangents, as indicated in Figure 5. The LCST of the PNIPAAm/chitosan hydrogel in this study was determined to be 33.08 °C and the peak temperature was close to a value 34.65 °C in the vicinity of the human body temperature.

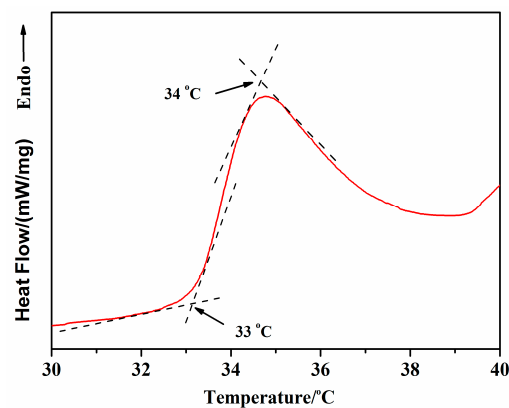


**Figure 5.** The LCST from a DSC thermogram of PNIPAAm/chitosan hydrogel.

### 3.3. Morphology of Nanofiber Mats

Figure 6 showed that the SEM micrographs of the temperature- and pH-sensitivity mulberry silk fabric before and after modified treatment with PNIPAAm/chitosan/PEO nanofibers. In contrast to the silk fabric (see Figure 6a), it can be seen from Figure 6b–d that the PNIPAAm/chitosan/PEO nanofibers overlap on the surface of silk fabrics, forming a coating. The results of SEM showed that the temperature- and pH-sensitivity mulberry silk fabric was successfully prepared with PNIPAAm/chitosan/PEO nanofibers by the electrospinning method. The higher porosity of the nanofiber mats and the smaller diameter of nanofibers were produced (see Figure 6b–d), which gave the silk fabric more temperature- and pH-responsive behaviors. It can be found from Figure 6e,f that the morphology of PNIPAAm/chitosan/PEO nanofibers produced no bead-like defects and a continuous, smooth surface.



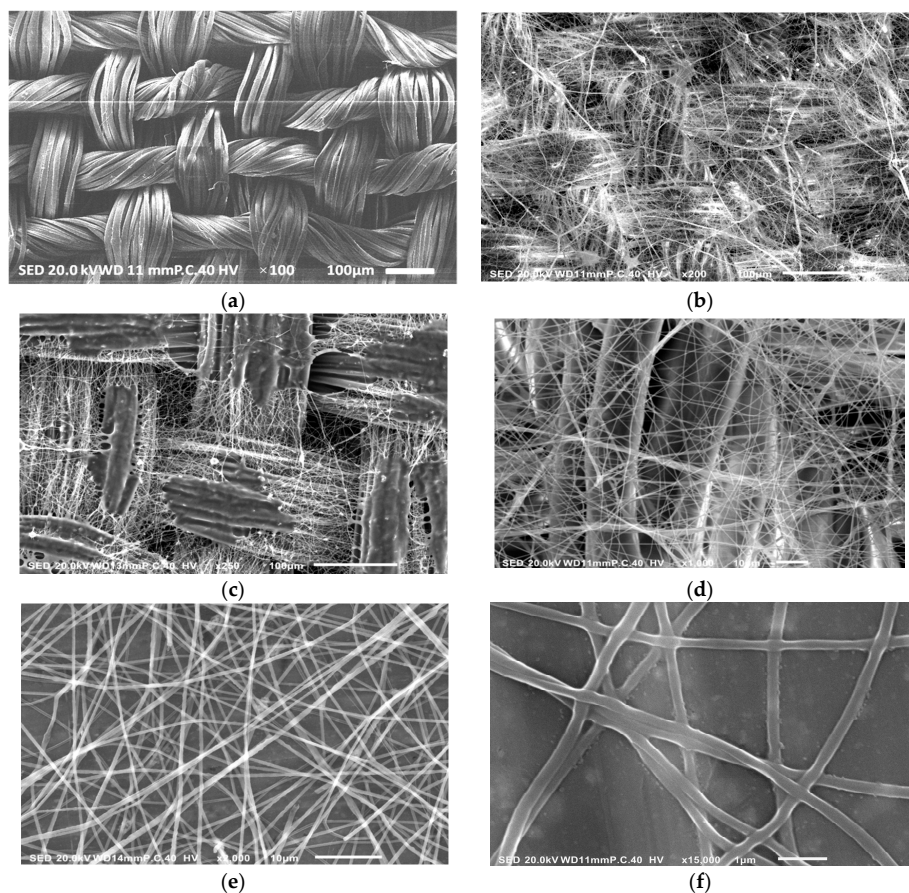


**Figure 6.** The morphology of (a) silk fabric, (b) temperature- and pH-sensitivity mulberry silk fabric ( $\times 200$ ), (c) temperature- and pH-sensitivity mulberry silk fabric ( $\times 250$ ), (d) temperature- and pH-sensitivity mulberry silk fabric ( $\times 1000$ ), (e) PNIPAAm/chitosan/PEO nanofibers ( $\times 1000$ ), and (f) PNIPAAm/chitosan/PEO nanofibers ( $\times 15,000$ ).

### 3.4. FT-IR Spectrum

Figure 7A presents the FT-IR spectra in the range from  $2000$  to  $500\text{ cm}^{-1}$ , which reflects comprehensively the NIPAAm powders, PNIPAAm powders, chitosan powders, PNIPAAm/chitosan hydrogel, and PNIPAAm/chitosan/PEO nanofibers. Infrared absorption spectra of the NIPAAm show characteristic absorption bands of the NIPAAm component assigned mainly to the double carbon bonds (C=C). The PNIPAAm powders give the characteristic absorption bands corresponding to the C=O stretching vibration. It can be seen from Figure 7A(a,b) that the appearance of the absorption spectra of NIPAAm at about  $1622\text{ cm}^{-1}$  corresponds to the C=C bond, wherein the absorption peak disappears by radical polymerization among NIPAAm monomers. It indicated that the NIPAAm monomer was successfully polymerized into products. Previous research work showed that the characteristic transmission peak of PEO attributed to the C–O–C stretching vibration presents at  $1095\text{ cm}^{-1}$  [33]. Moreover, this band is not disturbed by the mixture between PEO solution and PNIPAAm/chitosan solution (see Figure 7A(e)). As a result, poly(ethylene oxide) is appropriate to be used to improve the spinnability of PNIPAAm/chitosan.

Infrared spectroscopy was employed to investigate the molecular conformation of the PNIPAAm/chitosan/PEO nanofibers, temperature- and pH-sensitivity mulberry silk fabric and silk fabric. It is well-known that the glutaric dialdehyde can be separately reacted with chitosan and mulberry silk (see Figure 7B). By using a cross-linking agent, the aldehyde bonds (C=O) of glutaric dialdehyde separately reacted with the amine groups and hydroxyl bonds of chitosan and mulberry silk into the C=N and the C=C. The C=C, C=O and C=N produced a characteristic bands at  $3084$ ,  $1701$ ,

and  $1555\text{ cm}^{-1}$ , respectively, as we know the glutaric dialdehyde was volatile material. Thus, there are no extra glutaric dialdehyde in the resulting temperature- and pH-sensitivity mulberry silk fabric. And the Figure 7B(b) showed the intense peak at  $3084$ ,  $1701$ , and  $1555\text{ cm}^{-1}$ , suggesting that the reaction between the glutaric dialdehyde, chitosan, and the silk occurred. In contrast, there were no intense peaks at  $3084$ ,  $1701$ , and  $1555\text{ cm}^{-1}$  in the spectra of the PNIPAAm/chitosan/PEO nanofibers and silk fabric samples (Figure 7B(a,c)).

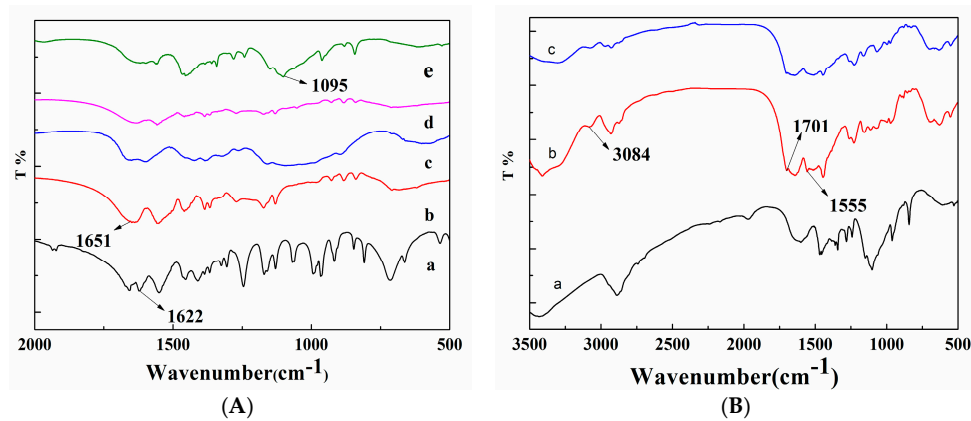


**Figure 7.** (A) The FT-IR spectra ( $500\text{--}2000\text{ cm}^{-1}$ ) of (a) NIPAAm powders, (b) PNIPAAm powders, (c) chitosan powders, (d) PNIPAAm/chitosan hydrogel, and (e) PNIPAAm/chitosan/PEO nanofibers. (B) The FT-IR spectra ( $500\text{--}3500\text{ cm}^{-1}$ ) of (a) PNIPAAm/chitosan/PEO nanofibers, (b) Temperature- and pH-sensitivity mulberry silk fabric, and (c) silk fabric.

### 3.5. Contact Angle

The hydrophilicity/hydrophobicity changes of the four groups of temperature- and pH-sensitivity mulberry silk fabrics were related to the structures of the modified silk fabric surface. The thermosensitive behavior was evaluated using a contact angle test apparatus. Contact angle images from the temperature- and pH-sensitivity mulberry silk fabric at different temperature and different times are shown in Figure 8. Figure 8A show that the contact angle of the modified cotton fabric at different temperature increases apparently with the rising temperature of the samples. There is a sudden increasing of the contact angle when the temperature was higher than  $35\text{ }^{\circ}\text{C}$ . It can be seen from Figure 8B that the contact angle of the modified cotton fabric at  $42\text{ }^{\circ}\text{C}$  had no obvious change in different time and retained about  $100^{\circ}$ . However, the contact angle of the modified cotton fabric at  $24\text{ }^{\circ}\text{C}$  was decreasing from  $30^{\circ}$  to  $0^{\circ}$ . The above results were attributed to the structures changes of the PNIPAAm on the modified silk fabric surface.

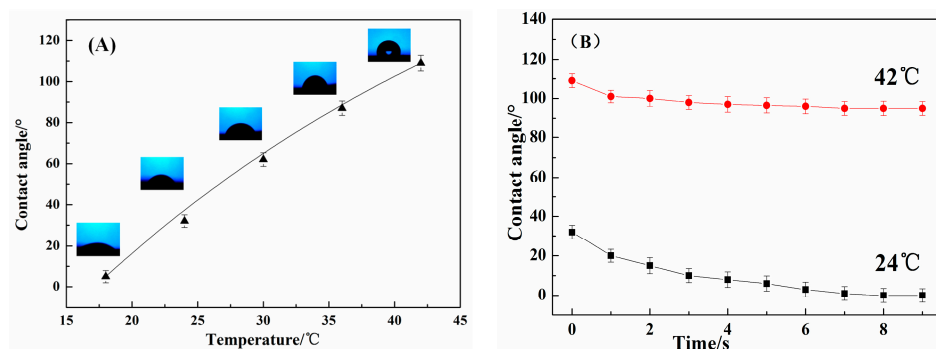


**Figure 8.** Contact angle measurements of temperature- and pH-sensitivity mulberry silk fabric: (A) at different temperature; (B) at different time. Data are presented as mean  $\pm$  standard deviation.



### 3.6. Air Permeability

Air permeability is described as the rate of air flow passing perpendicularly through a known area, under a prescribed air pressure differential between the two surfaces of a material. Tests were performed according to ISO 9237 [35], Determination of the Permeability of Fabrics to Air, using a Tex test FX-3300 air permeability tester. The pressure drop of 100 Pa and the test area 20 cm<sup>2</sup> were chosen for the measurement of air permeability to investigate the effect of the different conditions on the silk fabric.

As the control group, the four groups of coating silk fabrics were prepared with the PNIPAAm/chitosan/PEO solution and applied in the coating experiment at 30/60/90 min, respectively. The air permeability results of the temperature- and pH-sensitivity mulberry silk fabric modified with PNIPAAm/chitosan/PEO nanofibers with undertreated 30/60/90 min, respectively, silk fabric coated with PNIPAAm/chitosan/PEO solution and the silk fabric are shown in Figure 9.

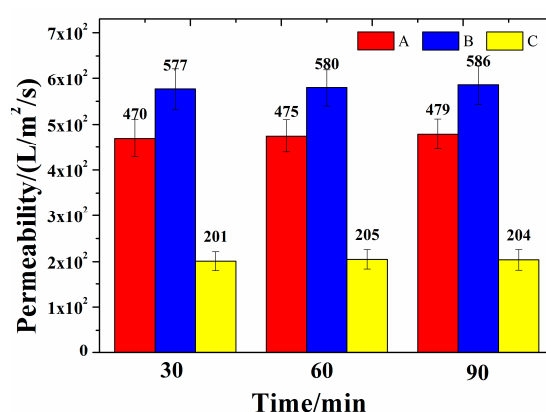


**Figure 9.** Air permeability of samples: (A) the temperature- and pH-sensitivity mulberry silk fabric modified with PNIPAAm/chitosan/PEO nanofibers; (B) silk fabric coated with PNIPAAm/chitosan/PEO solution; (C) mulberry silk fabric. Data are presented as mean  $\pm$  standard deviation.

According to Figure 9, it was found that the temperature- and pH-sensitivity mulberry silk fabric modified with PNIPAAm/chitosan/PEO nanofibers presented better performance results than that of the other silk fabric, with poorer air permeability. Moreover, the air permeability of temperature- and pH-sensitivity mulberry silk fabric modified with PNIPAAm/chitosan/PEO nanofibers showed no obvious change with the increasing of treatment duration, which has reached about  $5.1 \times 10^2$  L/m<sup>2</sup>/s. As a result, the performance of the temperature- and pH-sensitivity mulberry silk fabric modified with PNIPAAm/chitosan/PEO nanofibers has barely changed in terms of air permeability compared with the silk fabric. However, the air permeability of the silk fabric coated with PNIPAAm/chitosan/PEO solution only reaches  $1.5 \times 10^2$  L/m<sup>2</sup>/s. The method whereby the nanofibers modified the fabric has no effect on its permeability compared with the normal methods such as coating finishing. This is due to the distinctly high surface area to mass ratio and high porosity of the electrospinning nanofiber mats.

### 3.7. Antimicrobial Activity

The antibacterial efficiency of intellectualized thermoregulation silk fabric and silk fabric evaluated after the specific contact time and calculated by reduction percent of *E. coli* and *S. aureus* is shown in Table 1. It was found that the bacterial reduction rates of the silk fabric modified with nanofiber mats against *S. aureus* and *E. coli* have reached all above 80%, respectively—better than that of the untreated silk fabric, and silk fabric coated with PNIPAAm/chitosan/PEO solution. This may be due to the fact that the chitosan can restrain the bacteria's free movement, inhibit their respiration and eventually cause death. The electrostatic attraction between chitosan and bacteria would make the leakage of the intracellular components, including water and protein, and eventually lead to the destruction of the bacteria [36].

**Table 1.** Antibacterial activities of the silk fabrics.

Sample	<i>E. coli</i>		<i>S. aureus</i>	
	Surviving Cells	Reduction	Surviving Cells	Reduction
Unteated Mulberry Silk fabric	$2.3 \times 10^5$	–	$2.1 \times 10^5$	–
Silk fabric coated with PNIPAAm/chitosan/PEO solution	$2.8 \times 10^4$	88.26% $\pm$ 2%	$2.3 \times 10^4$	90% $\pm$ 2%
	$2.5 \times 10^4$		$2.0 \times 10^4$	
	$2.7 \times 10^4$		$2.1 \times 10^4$	
Temperature- and pH-sensitivity mulberry silk fabric	$2.2 \times 10^4$	90.43% $\pm$ 2%	$2.0 \times 10^4$	90.95% $\pm$ 2%
	$2.0 \times 10^4$		$1.9 \times 10^4$	
	$1.9 \times 10^4$		$1.8 \times 10^4$	

#### 4. Conclusions

The poly(*N*-isopropyl acrylamide) was synthesized in this paper at first; then the PNIPAAm was mixed with chitosan and poly(ethylene oxide) solution to obtain the electrospinning solution. Finally the electrospinning solution was electrospun to prepare the PNIPAAm/chitosan/PEO nanofiber for modifying the mulberry silk fabric. The modified silk fabric performed well in terms of thermosensitive behavior and pH-responsive swelling behaviors, antimicrobial activity and air permeability, suggesting it has a potential in functional textiles and intelligent materials.

**Acknowledgments:** This work was supported by Education Fund Item of Liaoning Province, Natural Science Fund of Liaoning province (2016341), Liaoning BaiQianWan Talents, Liaoning Provincial Key Laboratory of Functional Textile Materials and Liaoning Excellent Talents in University and Science.

**Author Contributions:** Yanhua Lu and Dehong Cheng conceived and designed the experiments; Jia Li and Boxiang Wang performed the experiments; Jia Li, and Jie Lin analyzed the data; Jia Li and Yanhua Lu wrote the paper.

**Conflicts of Interest:** The authors declare no conflict of interest.

#### References

- Hodak, S.K.; Supasai, T.; Paosawatyanong, B.; Kamlangklab, K.; Pavarajarn, V. Enhancement of the hydrophobicity of silk fabrics by SF 6, plasma. *Appl. Surf. Sci.* **2008**, *254*, 4744–4749. [[CrossRef](#)]
- Zhang, J. Silk fabrics modification through plasma graft copolymerization. *J. Text. Res.* **1996**, *4*, 1–4. (In Chinese)
- Kamlangkla, K.; Hodak, S.K.; Levalois-Grützmaier, J. Multifunctional silk fabrics by means of the plasma induced graft polymerization (PIGP) process. *Surf. Coat. Technol.* **2011**, *205*, 3755–3762. [[CrossRef](#)]
- Paosawatyanong, B.; Jermstujarit, P.; Bhanthumnavin, W. Graft copolymerization coating of methacryloyloxyethyl diphenyl phosphate flame retardant onto silk surface. *Prog. Org. Coat.* **2014**, *77*, 1585–1590.
- Lu, Z.; Zhang, H.; Zhou, M. Nano-functionalized silk for smart wearable devices. *Funct. Mater. Inf.* **2016**, *4*, 79. (In Chinese)
- Wang, C.; Li, X.; Gao, E.; Jian, M.; Xia, K.; Wang, Q.; Xu, Z.; Ren, T.; Zhang, Y. carbonized silk fabric for ultrastretchable, highly sensitive, and wearable strain sensors. *Adv. Mater.* **2016**, *28*, 6640–6648. [[CrossRef](#)] [[PubMed](#)]
- Cheng, C.; Teasdale, I.; Brüggemann, O. Stimuli-responsive capsules prepared from regenerated silk fibroin microspheres. *Macromol. Biosci.* **2014**, *14*, 807–816. [[CrossRef](#)] [[PubMed](#)]
- Stuart, M.A.C.; Huck, W.T.; Genzer, J.; Müller, M.; Ober, C.; Stamm, M.; Sukhorukov, G.B.; Szleifer, I.; Tsukruk, V.V.; Urban, M. Emerging applications of stimuli-responsive polymer materials. *Nat. Mater.* **2010**, *9*, 101–113. [[CrossRef](#)] [[PubMed](#)]
- Galaev, I.Y.; Mattiasson, B. “Smart” polymers and what they could do in biotechnology and medicine. *Trends Biotechnol.* **1999**, *17*, 335–340. [[CrossRef](#)]
- Schild, H.G. Poly(*N*-isopropylacrylamide): Experiment, theory and application. *Prog. Polym. Sci.* **1992**, *17*, 163–249. [[CrossRef](#)]
- Zhou, J.-X. Preparation of electromagnetic shielding textiles by sputtering/chemical coating technology. *Dyeing Finish.* **2008**, *5*, 1–6. (In Chinese)

12. Mao, C.; Guo, X.; Shi, D. Discussion on coating technology of wrapped rope in home textiles. *Shanghai Text. Sci. Technol.* **2011**, *29*, 27–28. (In Chinese)
13. Sonehara, M.; Sato, T.; Takasaki, M.; Konishi, H.; Yamasawa, K.; Miura, Y. Preparation and characterization of nanofiber nonwoven textile for electromagnetic wave shielding. *IEEE Trans. Magn.* **2008**, *44*, 3107–3110. [[CrossRef](#)]
14. Bhardwaj, N.; Kundu, S.C. Electrospinning: A fascinating fiber fabrication technique. *Biotechnol. Adv.* **2010**, *28*, 325–347. [[CrossRef](#)] [[PubMed](#)]
15. Greiner, A.; Wendorff, J.H. Electrospinning: A fascinating method for the preparation of ultrathin fibers. *Angew. Chem.* **2007**, *46*, 5670–5703. [[CrossRef](#)] [[PubMed](#)]
16. Shin, Y.M.; Hohman, M.M.; Brenner, M.P.; Rutledge, G.C. Experimental characterization of electrospinning: The electrically forced jet and instabilities. *Polymer* **2001**, *42*, 09955–09967. [[CrossRef](#)]
17. Subbiah, T.; Bhat, G.S.; Tock, R.W.; Parameswaran, S.; Ramkumar, S.S. Electrospinning of Nanofibers. *J. Appl. Polym. Sci.* **2005**, *96*, 557–569. [[CrossRef](#)]
18. Sill, T.J.; von Recum, H.A. Electrospinning: Applications in drug delivery and tissue engineering. *Biomaterials* **2008**, *29*, 1989–2006. [[CrossRef](#)] [[PubMed](#)]
19. Mitchell, G.R.; Davis, F. Electrospinning and Tissue Engineering. In *Advances on Modeling in Tissue Engineering*; Fernandes, P.R., Bártolo, P.J., Eds.; Springer: Dordrecht, The Netherlands, 2011; pp. 111–136.
20. Montazer, M.; Malekzadeh, S.B. Electrospun antibacterial nylon nanofibers through in situ synthesis of nanosilver: Preparation and characteristics. *J. Polym. Res.* **2012**, *19*, 1–6. [[CrossRef](#)]
21. He, J.; Wang, D.; Cui, S. Novel hydroxyapatite/tussah silk fibroin/chitosan bone-like nanocomposites. *Polym. Bull.* **2012**, *68*, 1765–1776. [[CrossRef](#)]
22. Guang, S.; An, Y.; Ke, F.; Zhao, D.; Shen, Y.; Xu, H. Chitosan/silk fibroin composite scaffolds for wound dressing. *J. Appl. Polym. Sci.* **2015**, *132*, 42503. [[CrossRef](#)]
23. Suh, J.-K.F.; Matthew, H.W.T. Application of chitosan-based polysaccharide biomaterials in cartilage tissue engineering: A review. *Biomaterials* **2000**, *21*, 2589–2598. [[PubMed](#)]
24. Lim, S.H.; Hudson, S.M. Application of a fiber-reactive chitosan derivative to cotton fabric as an antimicrobial textile finish. *Carbohydr. Polym.* **2004**, *56*, 227–234. [[CrossRef](#)]
25. Kumar, M.N.V.R. A review of chitin and chitosan applications. *React. Funct. Polym.* **2000**, *46*, 1–27. [[CrossRef](#)]
26. Chen, H.; Hsieh, Y.-L. Ultrafine hydrogel fibers with dual temperature-and pH-responsive swelling behaviors. *J. Polym. Sci. Part A Polym. Chem.* **2004**, *42*, 6331–6339. [[CrossRef](#)]
27. GB/T 31713-2015 *Hygienic Requirement for Safety of Antibacterial Textiles*; Standardization Administration of the People's Republic of China: Beijing, China, 2015. (In Chinese)
28. Wang, L.Y.; Ma, G.H.; Su, Z.G. Preparation of uniform sized chitosan microspheres by membrane emulsification technique and application as a carrier of protein drug. *J. Control. Release* **2005**, *106*, 62–75. [[CrossRef](#)] [[PubMed](#)]
29. Hadipour-Goudarzi, E.; Montazer, M.; Latifi, M.; Aghaji, A.A.G. Electrospinning of chitosan/sericin/PVA nanofibers incorporated with in situ synthesis of nano silver. *Carbohydr. Polym.* **2014**, *113*, 231–239. [[CrossRef](#)] [[PubMed](#)]
30. Lih, E.; Lee, J.S.; Park, K.M.; Park, K.D. Rapidly curable chitosan—PEG hydrogels as tissue adhesives for hemostasis and wound healing. *Acta Biomater.* **2012**, *8*, 3261–3269. [[CrossRef](#)] [[PubMed](#)]
31. Hu, X.; Lu, L.; Xu, C.; Li, X. Mechanically tough biomacromolecular IPN hydrogel fibers by enzymatic and ionic crosslinking. *Int. J. Biol. Macromol.* **2015**, *72*, 403–409. [[CrossRef](#)] [[PubMed](#)]
32. Jiang, C.; Wang, Q.; Wang, T. Thermoresponsive PNIPAAm-modified cotton fabric surfaces that switch between superhydrophilicity and superhydrophobicity. *Appl. Surf. Sci.* **2012**, *258*, 4888–4892. [[CrossRef](#)]
33. Lin, X.; Tang, D.; Cui, W.; Cheng, Y. Controllable drug release of electrospun thermoresponsive poly(*N*-isopropylacrylamide)/poly(2-acrylamido-2-methylpropane sulfonic acid) nanofibers. *J. Biomed. Mater. Res. Part A* **2012**, *100*, 1839–1845. [[CrossRef](#)] [[PubMed](#)]
34. Li, X.; Hsu, S.L. An analysis of the crystallization behavior of poly(ethylene oxide)/poly(methyl methacrylate) blends by spectroscopic and calorimetric techniques. *J. Polym. Sci. Part A Polym. Chem.* **2010**, *22*, 1331–1342. [[CrossRef](#)]

35. ISO 9237:1995 Textiles—Determination of the Permeability of Fabrics to Air; International Organization for Standardization: Geneva, Switzerland, 1995.
36. Lu, Y.; Cheng, D.; Lu, S.; Huang, F.; Li, G. Preparation of quaternary ammonium salt of chitosan nanoparticles and their textile properties on *Antheraea pernyi* silk modification. *Text. Res. J.* **2014**, *84*, 2115–2124. [[CrossRef](#)]



© 2018 by the authors. Licensee MDPI, Basel, Switzerland. This article is an open access article distributed under the terms and conditions of the Creative Commons Attribution (CC BY) license (<http://creativecommons.org/licenses/by/4.0/>).